

Phase-induced stability in a parametric dimer

Mauro Copelli and Katja Lindenberg

Department of Chemistry and Biochemistry 0340, University of California San Diego, La Jolla, California 92093-0340

(Received 1 August 2000; revised manuscript received 20 October 2000; published 20 February 2001)

We report results on a model of two coupled oscillators that undergo periodic parametric modulations with a phase difference θ . Being to a large extent analytically solvable, the model reveals a rich θ dependence of the regions of parametric resonance. In particular, the intuitive notion that antiphase modulations are less prone to parametric resonance is confirmed for sufficiently large coupling and damping. Some general results concerning synchronization properties in this system are presented. We also compare our results to a recently reported mean-field model of collective parametric instability, showing that the two-oscillator model captures much of the qualitative behavior of the infinite system.

DOI: 10.1103/PhysRevE.63.036605

PACS number(s): 45.05.+x, 05.45.Xt, 05.90.+m

I. INTRODUCTION

Parametric resonance is a phenomenon pervading several fields of science. It occurs when the modulation of a system parameter causes the system to become unstable. The literature on parametric resonance is enormous, so the best one can do is cite a range of different subjects where it may play a role. Examples include mechanical systems where such resonances were first identified [1–5], elementary particles [6], quantum dots [7], astrophysics [8], fluid mechanics [9], plasma physics [10], electronic networks [11], superconducting and laser devices [12], biomechanics [13], and even medicine [14]. Connections with chaotic systems have been suggested recently [15]. The simplest and perhaps most familiar example of parametric resonance occurs in a harmonic oscillator whose frequency varies periodically with time [1–5]. For certain ranges of modulation parameters (frequency, amplitude) the oscillator is unstable while for others it is stable. Even for this seemingly simple system the stability boundary diagram is already quite rich and complex (see below).

A great deal of recent work has dealt with systems of coupled oscillators—again, the literature in this general area is enormous. However, very little attention has focused on systems of coupled parametric oscillators [16,17]. Such coupled arrays are particularly intriguing because each single oscillator alone exhibits regions of stable or unstable behavior. Two questions arise naturally: (1) How does coupling modify the single-oscillator stability boundaries? (2) Are there collective parametric instabilities of the coupled system that are distinct from those experienced by single oscillators? In a recent paper Bena and Van den Broeck [16] addressed these questions for an infinite set of globally mean-field coupled harmonic oscillators subjected to time-periodic block pulses with quenched uniformly distributed random phases (“quenched” in this context means that the phase of the frequency modulation of each oscillator is set at time $t = 0$ and then remains unchanged). Within their mean-field treatment they are able to deal with both of the questions posed above. In particular, they find wide ranges of parameter values that lead to collective instabilities.

Our interest in this paper is to identify generic coupling

effects that are not specifically a consequence of the mean-field analysis, and in this context to understand how a coupled system of (very) few oscillators with short-ranged interactions might carry in it the seeds of the infinite/infinately cross-coupled array. In particular, we seek the seeds of the collective parametric instabilities. We do this by studying a model of two coupled oscillators. The control parameter is the phase difference in the periodic modulation of the frequencies of the two oscillators.

In Sec. II we introduce the general model, while in Sec. III we specialize to a particular model that admits a partially analytic solution. Section IV is a presentation of results as a collection of stability boundary diagrams that convey the way in which stability boundaries shift, appear, and disappear with parameter changes. In Sec. V we analyze the ways in which the seeds of the collective parametric instabilities found in the mean-field model already appear in the two-oscillator system. A brief summary of our conclusions is reiterated in Sec. VI.

II. PARAMETRIC DIMER

Our system consists of two linearly coupled parametric oscillators whose equations of motion are

$$\begin{aligned}\ddot{x}_1 &= -\omega_0^2[1 + \phi_1(t)]x_1 - k(x_1 - x_2) - \gamma\dot{x}_1, \\ \ddot{x}_2 &= -\omega_0^2[1 + \phi_2(t)]x_2 - k(x_2 - x_1) - \gamma\dot{x}_2.\end{aligned}\tag{1}$$

Here ω_0 is the natural frequency of each (uncoupled) oscillator, k is the coupling constant between them, and γ is the damping coefficient. The parametric modulations $\phi_1(t)$ and $\phi_2(t)$ are periodic with period $T \equiv 2\pi/\omega_p$ and are identical except for a phase difference θ , that is, $\phi_2(t) = \phi_1(t + \theta/\omega_p)$. In the absence of the frequency modulation one is left with coupled ordinary damped harmonic oscillators whose total energy decays exponentially to zero. In the presence of the parametric modulation, however, energy is periodically pumped into the system, which may or may not lead to parametric resonance, i.e., to an infinite growth of the amplitudes of the oscillators. Our goal is to determine the boundaries between these two behaviors, which will be re-

ferred to as “unstable” and “stable.” We carry out the detailed plan for a particular modulation but obtain results that can be generalized beyond this specific case.

The linearity of the equations allows one to make use of Floquet theory to solve the problem [4]. Defining

$$\mathbf{X} \equiv \begin{pmatrix} x_1 \\ \dot{x}_1 \\ x_2 \\ \dot{x}_2 \end{pmatrix}, \quad (2)$$

one can rewrite Eqs. (1) in matrix form as $\dot{\mathbf{X}}(t) = \hat{D}(t)\mathbf{X}(t)$ with a matrix \hat{D} satisfying $\hat{D}(t) = \hat{D}(t+T)$. Given a solution $\mathbf{X}(t)$, the time periodicity of the parametric modulations thus implies that $\mathbf{X}(t+T)$ is also a solution. Therefore one can find a matrix \hat{F} such that

$$\mathbf{X}(t+T) = e^{-2\gamma T} \hat{F}(T) \mathbf{X}(t) \quad (3)$$

and hence more generally through a repetition of this solution

$$\mathbf{X}(t+nT) = e^{-2n\gamma T} \hat{F}^n(T) \mathbf{X}(t). \quad (4)$$

The long-time behavior of the system is thus clearly determined by the eigenvalues $\{\lambda_i\}$ of the *Floquet operator* $e^{-2\gamma T} \hat{F}$, which propagates the system in phase space for one period of the modulation. The eigenvalues obey the relation

$$\prod_{i=1}^4 \lambda_i = e^{-2\gamma T} \quad (5)$$

reflecting the incompressible flow in the absence of damping. The eigenvectors \mathbf{v}_j of $e^{-2\gamma T} \hat{F}$ satisfy $|\mathbf{v}_j(t+nT)| = |\lambda_j|^n |\mathbf{v}_j(t)|$, so in the limit $n \rightarrow \infty$ parametric resonance occurs if $\max_j \{|\lambda_j|\} > 1$.

Explicit solution of the problem requires specification of the modulation, and in the next section we choose a particular form that allows a partially analytic solution. However, there are some general features of behavior that can be established independently of the particular modulation, as long as it is periodic and the same (except for a phase difference) for the two oscillators. These general features are particularly interesting in the context of synchronization phenomena.

For in-phase modulation ($\theta = 0$), $\phi_2(t) = \phi_1(t)$ and it becomes possible to reduce the original four-dimensional problem to two two-dimensional systems. This decoupling is accomplished by changing the coordinate system to the reference frame of the center of mass. Defining $x \equiv (x_1 + x_2)/2$ and $\rho \equiv (x_1 - x_2)$, one obtains from Eq. (1)

$$\ddot{x} = -\omega_0^2 [1 + \phi_1(t)]x - \gamma \dot{x}, \quad (6)$$

$$\ddot{\rho} = -\{\omega_0^2 [1 + \phi_1(t)] + 2k\}\rho - \gamma \dot{\rho}. \quad (7)$$

Each of these equations is precisely that of a *single* parametric oscillator, one with frequency ω_0 and the other with fre-

quency $\omega'_0 = (\omega_0^2 + 2k)^{1/2}$, both with modulation $\phi_1(t)$. This greatly simplifies the problem since the solutions to the single-oscillator problem are well known [1–5] (sometimes in full analytical detail) for some choices of the function $\phi_1(t)$. In particular, the regions of instability of the dimer system consist of the union of those of each of the single oscillators. This immediately allows some general observations: (1) Since x in Eq. (6) corresponds *exactly* to either of the single oscillators in Eq. (1) with k set to zero, it is clear that for any nonzero k , due to the added ρ instabilities, the dimer will become more unstable than an originally uncoupled system; (2) since each of the single oscillators in Eqs. (6) and (7) can become unstable, it is possible for the oscillators in the dimer to become *synchronously* unstable [if the amplitude of $x(t)$ diverges but that of $\rho(t)$ does not] or *antisynchronously* unstable [if the amplitude of $\rho(t)$ diverges but that of $x(t)$ does not].

We now consider antiphase modulation ($\theta = \pi$) with $\phi_2(t) = -\phi_1(t)$ (odd parity modulation). This turns out to be a very interesting case for a number of reasons presented in the context of the specific system chosen below, but it can be said in general that neither synchronization nor antisynchronization is possible. This is easily seen from the equations of motion, which do not admit the solutions $x_2 = \pm x_1$ in this case. In fact, this result can be further generalized to nonlinear systems as well. Assume that a parametric dimer evolves according to the equations of motion $\ddot{x}_{1,2} = -[1 + \phi_{1,2}(t)]Y(x_{1,2}) - \Xi(x_{1,2} - x_{2,1}) - \Gamma(\dot{x}_{1,2})$, where Y characterizes each oscillator, Ξ accounts for the coupling between the oscillators, and Γ represents damping. Y , Ξ , and Γ can be *any* odd functions (thus possibly nonlinear), the only restriction being that Y is nonzero if its argument is nonzero. Under these conditions (with ϕ_1 and ϕ_2 related as above) one can easily verify that $x_2 = \pm x_1 \Rightarrow x_1(t) = x_2(t) = 0$. On physical grounds this is a reasonable result, since the antiphase of the parametric modulation amounts to a permanent frequency mismatch between the two oscillators.

III. SQUARE WAVE MODULATION

We concentrate on a square wave modulation of period $T = 2\pi/\omega_p$ and amplitude A :

$$\phi_1(t) = A \operatorname{sgn}[\sin(\omega_p t)], \quad (8)$$

$$\phi_2(t) = A \operatorname{sgn}[\sin(\omega_p t + \theta)].$$

This choice is appealing because for any number of oscillators (a single oscillator, or the coupled oscillators considered here, or even the mean-field version of an infinitely cross-coupled infinite chain [16]) the piecewise constant parametric modulation leads to a piecewise linear system whose piecewise solution is known analytically. One can therefore construct the Floquet operator explicitly by simply multiplying together *piecewise linear Floquet operators*. This provides an immense reduction in computational effort by skipping what is usually the most time-consuming task in

obtaining the regions of parametric resonance, namely, the numerical evaluation of the Floquet operator itself. For an isolated oscillator this procedure is well known [1,3,5]. It is worth noting that a simple rescaling of time to dimensionless units, $t' = t\omega_0$, shows that Eqs. (1) with this modulation are governed by the dimensionless parameter combinations $r \equiv \omega_0/\omega_p$, $A, k/\omega_0^2$, γ/ω_0 , and θ . Moreover, the behavior of the system is invariant with respect to the replacement of θ by $\theta' \equiv 2\pi - \theta$ (reflection around π) since this just amounts to an exchange of indices between the oscillators.

For the sake of clarity, let us first analyze the frictionless case $\gamma=0$. Each linear interval is characterized by one of the four possible states of the modulations $(\phi_1, \phi_2) = (+A, +A), (+A, -A), (-A, +A),$ or $(-A, -A)$. For each of these states, the solutions are of the form $X_j(t) = A_j^{(+)} e^{iPt} + A_j^{(-)} e^{-iPt} + B_j^{(+)} e^{iMt} + B_j^{(-)} e^{-iMt}$, where the eigenfrequencies P and M follow directly from the diagonalization of the matrix \hat{D} associated with that state:

$$P^2 = \frac{\omega_1^2 + \omega_2^2 + \sqrt{(\omega_1^2 - \omega_2^2)^2 + 4k^2}}{2},$$

$$M^2 = \frac{\omega_1^2 + \omega_2^2 - \sqrt{(\omega_1^2 - \omega_2^2)^2 + 4k^2}}{2},$$
(9)

where $\omega_{1,2}^2 \equiv \omega_0^2[1 + \phi_{1,2}(t)] + k$. Denoting the current state of the modulation by indices $+$ and $-$, notice that while $P_{++}, M_{++},$ and $P_{+-} = P_{-+}$ are always real, M_{--} becomes imaginary when $A > 1$ while P_{--} and $M_{+-} = M_{-+}$ become imaginary when $A > 1 + 2k/\omega_0^2$ and $A > (1 + 2k/\omega_0^2)^{1/2}$, respectively. Whether the system periodically alternates between harmonic behavior and one or more saddle nodes will thus depend on the parameter region and the phase difference θ .

During a time interval τ with fixed ϕ_1, ϕ_2 we can relate $\mathbf{X}(t + \tau)$ to $\mathbf{X}(t)$ as $\mathbf{X}(t + \tau) = \hat{f}(\tau)\mathbf{X}(t)$, where \hat{f} is the *piecewise* linear Floquet operator:

$$\hat{f}(t) = \frac{1}{P^2 - M^2} \begin{pmatrix} -m_1 c_p + p_1 c_m & -m_1 s_p + p_1 s_m & k[-c_p + c_m] & k[-s_p + s_m] \\ m_1 P^2 s_p - p_1 M^2 s_m & -m_1 c_p + p_1 c_m & k[P^2 s_p - M^2 s_m] & k[-c_p + c_m] \\ k[-c_p + c_m] & k[-s_p + s_m] & -m_2 c_p + p_2 c_m & -m_2 s_p + p_2 s_m \\ k[P^2 s_p - M^2 s_m] & k[-c_p + c_m] & m_2 P^2 s_p - p_2 M^2 s_m & -m_2 c_p + p_2 c_m \end{pmatrix},$$
(10)

where we make use of the shorthand notation $c_p \equiv \cos(Pt)$, $s_p \equiv P^{-1} \sin(Pt)$, $c_m \equiv \cos(Mt)$, $s_m \equiv M^{-1} \sin(Mt)$, $m_{1,2} \equiv M^2 - \omega_{1,2}^2$, and $p_{1,2} \equiv P^2 - \omega_{1,2}^2$. The Floquet operator is then finally obtained as the product of piecewise Floquet operators with arguments that depend on the phase difference between the modulations:

$$\hat{F}(T) = \hat{f}_{-+} \left(\frac{T}{2} \frac{\theta}{\pi} \right) \hat{f}_{--} \left(\frac{T}{2} \left[1 - \frac{\theta}{\pi} \right] \right) \times \hat{f}_{+-} \left(\frac{T}{2} \frac{\theta}{\pi} \right) \hat{f}_{++} \left(\frac{T}{2} \left[1 - \frac{\theta}{\pi} \right] \right).$$
(11)

The stability properties of the coupled system are determined by the magnitudes of the four eigenvalues $\lambda_1, \dots, \lambda_4$ of the Floquet operator. Note that, if $\theta=0$ or $\theta=\pi$, the above expression reduces to the product of only two matrices (as it should) since $\hat{f}(0)$ is just the identity matrix. If damping is present then the variables $y_i = e^{\gamma t/2} x_i$ obey equations identical to those of the undamped system but with the shift $\omega_{1,2}^2 \rightarrow \omega_{1,2}^2 - \gamma^2/4$. The inclusion of damping is thus a simple matter.

IV. RESULTS

For a single parametric oscillator Eq. (5) involves only two eigenvalues and the product condition is sufficient to

determine the location of the parametric resonance boundaries [5]:

$$\cos\left(\frac{\tilde{\omega}_- T}{2}\right) \cos\left(\frac{\tilde{\omega}_+ T}{2}\right) - \left(\frac{\tilde{\omega}_+^2 + \tilde{\omega}_-^2}{2\tilde{\omega}_+ \tilde{\omega}_-}\right) \times \sin\left(\frac{\tilde{\omega}_- T}{2}\right) \sin\left(\frac{\tilde{\omega}_+ T}{2}\right) = \pm \cosh\left(\frac{\gamma T}{2}\right),$$
(12)

where $\tilde{\omega}_{\pm}^2 \equiv \omega_0^2(1 \pm A) - \gamma^2/4$. This equation defines the points at which one of the eigenvalues equals either $+1$ or -1 . In the absence of damping the solutions depend only on A and the ratio $r \equiv \omega_0/\omega_p$, and these particular results are shown by the dashed curves in the first panel of Fig. 1. The regions of instability appear as ‘‘tongues’’ starting from integer and half-integer values of r at small modulation amplitudes. Note that no abrupt transition (nor a visible transition of any kind) is seen at the line $A=1$ which marks the transition between an oscillating-oscillating behavior and a saddle-oscillating one [5]. As one would expect, on the other hand, the system is nearly always unstable for sufficiently small ω_p and sufficiently large A (upper right corner of the figure).

In contrast with the single oscillator, relation (5) for the coupled oscillators is not a sufficient condition to guarantee

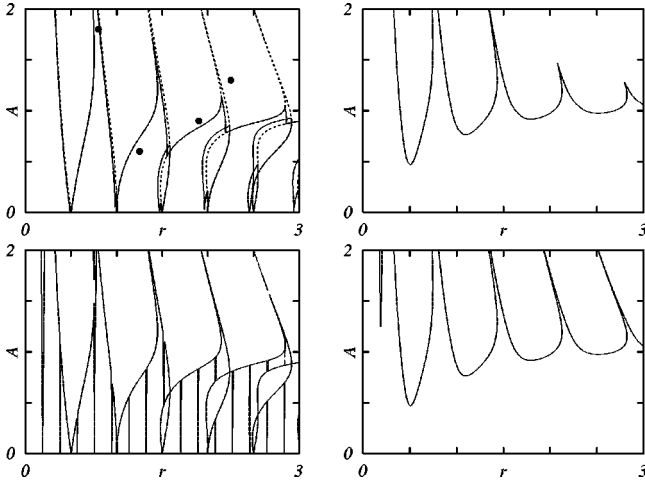


FIG. 1. Instability boundaries for $\theta=0$ in the (r, A) plane. $\gamma = 0$ in the first column while $\gamma/\omega_0=0.3$ in the second column. $k/\omega_0^2=0.02$ in the first row, while $k/\omega_0^2=3$ in the second row. The dashed line in the first panel is the result for $k=0$ (single uncoupled oscillator). The dark points in this panel are parameter pairs to be considered in more detail subsequently.

that the parametric resonance bifurcations occur when at least one eigenvalue is $\lambda_j = \pm 1$ [3–5]: for coupled oscillators the largest eigenvalue can cross the unit circle $|\lambda_j|=1$ and hence enter a region of instability (parametric resonance) in other directions in the complex plane. The fourth order characteristic polynomial must be solved numerically to determine the instability boundaries; this is still a computationally inexpensive procedure since we have an analytic expression for the Floquet operator.

A. In-phase modulations

When $\theta=0$, corresponding to in-phase modulation, each of the two equations (6) and (7) is precisely that of a single parametric oscillator, one with frequency ω_0 and modulation amplitude A , the other with rescaled parameters

$$\begin{aligned}\omega'_0 &\equiv \sqrt{\omega_0^2 + 2k}, \\ A' &\equiv A(\omega_0/\omega'_0)^2.\end{aligned}\quad (13)$$

We can thus use the known results for the single oscillator [1,3,5], for which the closed expression (12) gives the boundaries of the instability regions in the (r, A) plane. The instability regions for the dimer are given by the union of the sets of tongues arising from each independent oscillator, one set emerging from integer and half-integer values of r (“ r -instability regions”), and the other from

$$r'(k) \equiv r\sqrt{1 + 2k/\omega_0^2} = \frac{\omega'_0}{\omega_p} \quad (14)$$

(“ r' -instability regions”). When the coupling k between the oscillators is small the two sets of tongues almost overlap and one obtains in the undamped case the solid curves in the first panel of Fig. 1, which show the instability boundaries

when $k/\omega_0^2=0.02$. Still in the undamped problem, when the coupling k is large the two sets of tongues occur at different parameter scales. The boundary diagram for $k/\omega_0^2=3$ is shown in the lower left panel of the figure. In either case, since now we have two independent sets of instability regions the effect of the coupling k for $\theta=0$ has been to *enlarge* the parametric resonance regime relative to that of two uncoupled oscillators. As mentioned earlier, this is a general result regardless of the form of the periodic modulation. The details of the phase boundaries do of course depend on the specific modulation function.

Damping, even in an isolated parametric oscillator, destroys much of the intricate boundary structure and increases the regions of stability. This is also the case for coupled oscillators, where increasing the damping tends to blur out the effects of coupling. These behaviors can be seen in the right column of Fig. 1. The regions of instability are now restricted to larger amplitudes A . Note the similarity between these two figures, which involve different couplings but now with substantial damping, $\gamma/\omega_0=0.3$. Note also that in the lower panel of this column (large coupling) the very first instability wedge is an r' -instability region while the other portions of the diagram (as well as the unstable regions in the upper weak-coupling case) include both r and r' instabilities.

For $\theta=0$ these results allow us to say something about the interesting problem of asymptotic synchronization in light of the general results already expressed in Sec. II. In regions where the center of mass coordinate x is unstable but the relative coordinate ρ is stable (r -instability regions that do not overlap with r' -instability regions) the coupled oscillators are synchronized if $\gamma \neq 0$ ($x_1=x_2$), that is, the two oscillators move together about the origin with ever increasing amplitude. Conversely, if x is stable but ρ is unstable (r' -instability regions that do not overlap with r -instability regions), with $\gamma \neq 0$ the oscillators become “antisynchronized” ($x_1=-x_2$), that is, the two oscillators oscillate with ever increasing amplitude but in opposite directions, crossing one another each time they pass through the origin. Antisynchronization becomes more difficult to achieve with increasing coupling. If $\gamma=0$ the strict equalities $x_1=x_2$ or $x_1=-x_2$ no longer hold in the nonoverlapping regions, but the difference between x_1 and x_2 or $-x_2$ is oscillatory and remains bounded. A simultaneous instability of both x and ρ involves an unstable center of mass coordinate and unbounded oscillations of each oscillator about this unbounded mean, which in turn involves a more complicated phase relation between the motions of the two oscillators. We return to this issue later.

B. Out-of-phase modulations

A wealth of very intricate results arises when $\theta \neq 0$. In contrast with the $\theta=0$ case, it is now no longer clear how to break down the problem into simpler independent components (even for $\theta=\pi$) and, in particular, there is no longer a transparent way to relate the results to those of single parametric oscillators. The only way to convey the intricacy of the problem appears to be graphical, and so we present an array of results in the next few figures. Since there are sev-

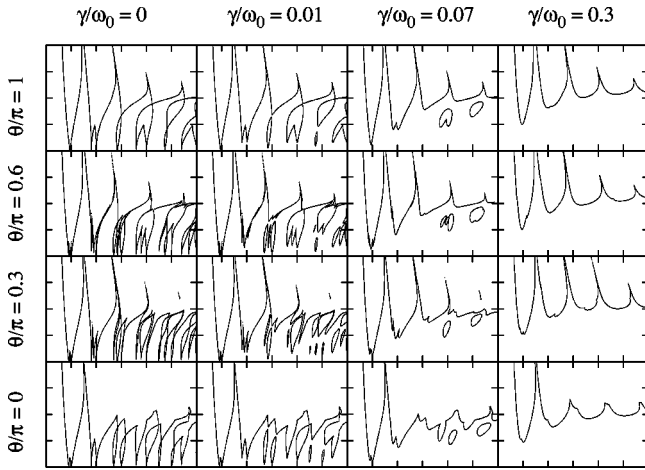


FIG. 2. (r, A) plane as in Fig. 1 for $k/\omega_0^2=0.12$ and several combinations of θ and γ (origin is at bottom left corner; tick marks are separated by half a unit on each axis).

eral parameters that sensitively affect the instability boundaries, comparisons within and among figures are required.

Perhaps the most striking feature of the θ dependence is its sensitivity: the unstable regions in the (r, A) plane can change very abruptly (yet continuously) with the phase difference. As one might expect, this sensitivity is strongly modulated by the coupling k . This is clearly seen by comparing one by one the corresponding panels in Figs. 2 and 3. These figures show the instability regions in the (r, A) plane for various parameter combinations, but with the coupling constant fixed within each figure [in order to save space, these and subsequent figures consistently omit labels, using the same scale as Fig. 1 in the (r, A) plane, with the origin at the bottom left corner and tick marks separated by half a unit on both axes]. Without dwelling on the details at this point, it is clear that the corresponding panels for stronger coupling present a more intricate boundary pattern. Figures 2 and 3 are tiled so as to exhibit most clearly the effects of damping and of the modulation phase difference. In these renditions θ

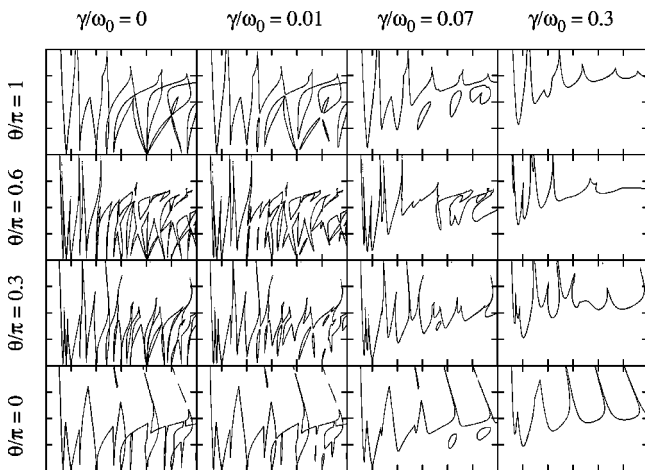


FIG. 3. (r, A) plane as in Fig. 1 for $k/\omega_0^2=0.6$ and several combinations of θ and γ (origin is at bottom left corner; tick marks are separated by half a unit on each axis).

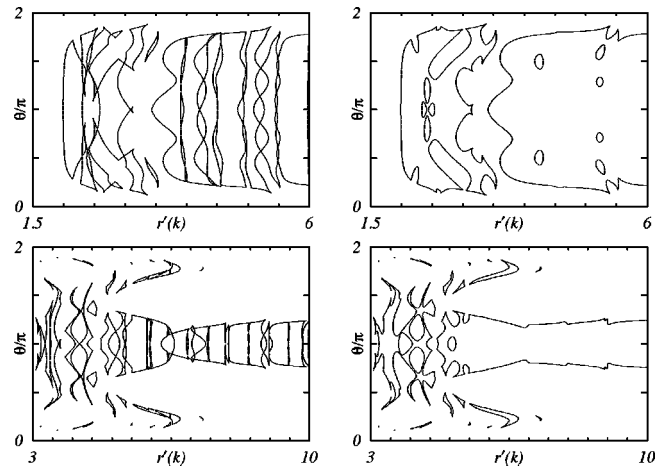


FIG. 4. Stability regions in the (k, θ) plane in the absence (left column, $\gamma=0$) or presence (right column, $\gamma/\omega_0=0.05$) of damping. Top panels: $r=1.9$ and $A=0.9$. Bottom panels: $r=2.25$ and $A=1.3$.

varies in the vertical direction while γ varies in the horizontal direction. Figure 2 shows such a panel for a relatively small coupling $k/\omega_0^2=0.12$. One notices that the θ dependence is smoothed out as damping increases, so that almost no structure is visible along the rightmost column ($\gamma/\omega_0=0.3$). Figure 3 shows the results for a larger coupling $k/\omega_0^2=0.6$. Note that the same tendency is observed: the instability boundaries become gradually less sensitive to θ as γ increases. However, the rightmost column of Fig. 3 now shows much more structure than that of Fig. 2, indicating that for the same value of γ the (r, A) plane with larger k shows a stronger θ dependence.

Figures 2 and 3 suggest that $\theta=\pi$ gives rise to particularly stable behavior. This is in agreement with the intuitive notion that antiphase modulations should be less prone to resonance than in-phase ones. In order to verify this intuition, a complementary view of these phenomena can be obtained by instead projecting the instability regions in the (k, θ) plane. This allows us to start with uncoupled oscillators ($k=0$) and observe how a given (in)stability evolves as k and θ change. Indeed, it turns out to be possible to understand much of the behavior of the coupled system in terms of the behavior of the uncoupled system. To produce the representative results shown in Figs. 4 and 5, we fix several (r, A) points in the single-oscillator stability boundary diagram shown as black circles in the first panel of Fig. 1 and study the way in which variations in k and θ affect these particular states. Two of the points in Fig. 1, $(r, A)=(0.8, 1.8)$ and $(1.25, 0.6)$, are stable states for the single oscillator (the first black dot touches the stability boundary in the figure only because it has been drawn large enough to render it visible; the point is well within the stable region). The other two points, $(r, A)=(1.9, 0.9)$ and $(2.25, 1.3)$, lead to unstable behavior of the single oscillator.

The first thing to be noted in Fig. 4 is that the horizontal axis has been rescaled in order to reveal the relevance of the variable r' [see Eq. (14)]. The top panels focus on $r=1.9$ and $A=0.9$, which is in the parametrically resonant regime

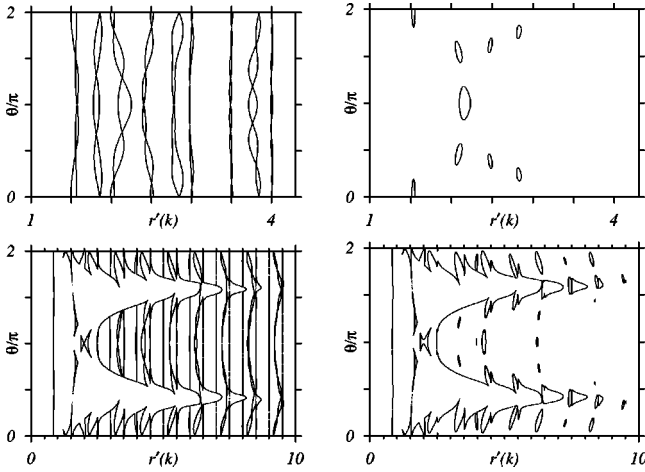


FIG. 5. Instability regions in the (k, θ) plane in the absence (left column, $\gamma=0$) or presence (right column, $\gamma/\omega_0=0.05$) of damping. Top panels: $r=1.25$ and $A=0.6$. Bottom panels: $r=0.8$ and $A=1.8$.

for the uncoupled system. The small- r' portion of the figure thus represents an unstable regime. One notes that for $r'(k)$ slightly above 2 the system becomes stable within a θ interval centered around π . Increasing k a little further, this stability region then evolves in a very complex pattern, which includes reentrant “holes” of instability. After a distinguishable gap of instability, a somewhat simpler band of stability arises around $r' \sim 3.5$ starting at $\theta = \pi$. This band continues to larger values of k , with its outermost boundaries presenting a relatively simpler envelope than the low- k pattern. The interesting point to be emphasized is that the band is perforated by gaps of instability most of which are centered precisely at integer and half-integer values of r' . This result is perhaps anticipated by the fact that the frequency ω_0' appears as the effective average diagonal frequency in the mean-field equation of motion in Ref. [16]. The gaps are eventually closed by increasing the damping (top right panel), which also broadens the stability band and simplifies its dependence on the phase difference. The bottom panels in Fig. 4 are for $r=2.25$ and $A=1.3$, which again is in the resonant regime of the single oscillator. One notices the same pattern: for lower values of k a complex shape emerges in the θ dependence of the stable regions. For sufficiently large values of k , a band of stability arises which has instability gaps basically centered at integer and half-integer values of r' . Damping (bottom right panel) causes gaps to disappear, creating a uniform region of stability centered around $\theta = \pi$.

Figure 5 presents what may be regarded as the opposite situation, namely, when the original uncoupled system is stable. The top panels show the results for $r=1.25$ and $A=0.6$. Notice that the behavior is much simpler in this case, with the original stability being disturbed mostly around integer and half-integer values of r' in the absence of damping (top left), with a relatively weak θ dependence. The effect of damping (top right) is to suppress most of these instability regions, yielding a predominantly stable (k, θ) plane. The bottom panels show results for an interesting intermediate situation: even though the uncoupled system is stable for

$=0.8$ and $A=1.8$, this point lies in a narrow corridor between two instability regions in the (r, A) plane (see Fig. 1). One would therefore expect instabilities to arise more easily, and the immediate question is how the resulting diagram might reconcile the structures observed in Fig. 4 and the top panels of Fig. 5. The answer lies in a very rich structure in the (k, θ) plane (bottom left panel): initially, very small coupling induces an instability for all θ . The now predominantly unstable system evolves in a manner similar to those of Fig. 4, a stability region being created around $\theta = \pi$ as k increases, with stringlike gaps of instability around the usual values of r' . The difference is that there is now also a usual band of stability centered around $\theta = 0$, presenting gaps at the same r' positions. For k sufficiently large, those two stability bands merge and one is left with a structure similar to that of the top panels: a predominantly stable region permeated by strings of instability. The bottom right panel of Fig. 5 shows the effect of damping, which significantly reduces the instability gaps, thus greatly simplifying the picture.

The notion that modulations operating with a phase difference $\theta = \pi$ are less prone to parametric resonance is thus seen to be essentially correct. Framing this statement more carefully, our results show that, for given r and A , sufficiently large values of k/ω_0^2 and γ/ω_0 are able to induce, in the (k, θ) plane, a band of stability centered around $\theta = \pi$ even if the uncoupled oscillators are individually unstable. The width of this band can eventually comprise the whole 2π interval if the uncoupled system is originally stable.

V. COLLECTIVE PARAMETRIC INSTABILITY

Bena and Van den Broeck [16] studied the stability boundaries of N parametrically modulated oscillators $\{x_i\}$ each coupled to all the others by the same coupling constant $2k/N$ (in our notation). The phases $\{\theta_i\}$ are initially chosen at random from a uniform distribution in the interval $[0, 2\pi]$, remaining quenched thereafter. With a square block modulation the system is exactly solvable in the limit $N \rightarrow \infty$, where the mean-field solution becomes exact. The mean-field equation is

$$\ddot{x} = -\omega_0^2 [1 + \phi_\theta(t)]x - \gamma \dot{x} - 2k(x - \langle x \rangle), \quad (15)$$

where x is the displacement of any oscillator in the chain, $\phi_\theta(t)$ is the periodic modulation with phase θ , and $\langle x \rangle \equiv N^{-1} \sum_{i=1}^N x_i$ is the mean displacement to be determined self-consistently. Bena and Van den Broeck note that the exact solution of this equation is

$$\begin{pmatrix} x(t) \\ \dot{x}(t) \end{pmatrix} = \mathbf{G}_\theta(t) \cdot \begin{pmatrix} x(0) \\ \dot{x}(0) \end{pmatrix} + 2k \mathbf{G}_\theta(t) \cdot \int_0^t d\tau \mathbf{G}_\theta(\tau)^{-1} \cdot \begin{pmatrix} 0 \\ \langle x(\tau) \rangle \end{pmatrix}. \quad (16)$$

The propagator $\mathbf{G}(t)$ is known explicitly. Indeed, at $t=T$ it is $\mathbf{G}(T) = e^{-\gamma T} \hat{F}(T)$ where \hat{F} is precisely the single-oscillator

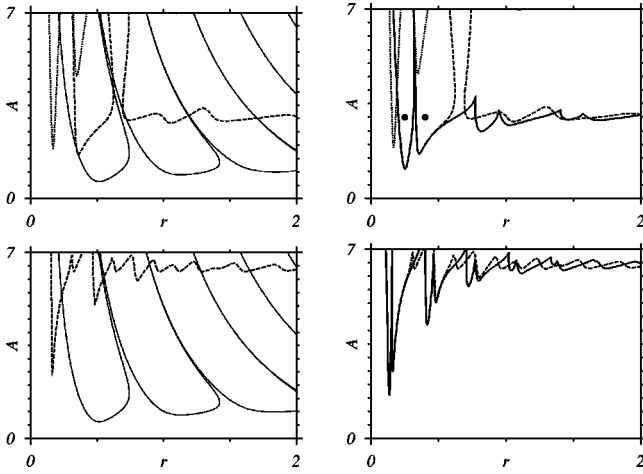


FIG. 6. Instability regions in the (r, A) plane for $\gamma/\omega_0=0.4$. According to the mean-field model [16], the usual parametric resonance occurs inside the dotted boundaries, while the boundaries of collective instability are depicted by dashed lines. $k/\omega_0^2=4$ for the top panels, and $k/\omega_0^2=20$ for the bottom panels. The thin solid lines correspond to $k=0$ (left column); the thick solid lines (right column) correspond to $\theta=\pi$ in the two-oscillator model. The dark points in the upper right panel are parameter pairs considered in more detail subsequently.

Floquet operator with the frequencies appropriately shifted by the coupling constant. Note that this is *exactly* the same as the propagator associated with the ρ variable of Eq. (7) in the two-oscillator in-phase modulation problem, that is, the propagator associated with a single oscillator of frequency ω'_0 .

Bena and Van den Broeck identify two sorts of instabilities. One, which they call the “usual parametric resonance,” arises from the divergence associated with eigenvalues of \mathbf{G} of magnitude greater than unity, that is, with the unbounded growth of the first term in Eq. (16), which in turn signals the unbounded growth of the amplitude of any typical oscillator in the chain. The stability boundaries associated with this type of instability are given precisely by Eq. (12) and are shown for the parameter choices indicated in the caption as the dotted curves in the top row panels of Fig. 6. In our in-phase two-oscillator parlance these are exactly the boundaries of the “ r' -instability regions” defined in terms of the shifted frequency ω'_0 [cf. Eq. (13)]. The “usual” regions shrink in width and move toward lower r and larger A with increasing coupling k , a behavior already exhibited in the context of the in-phase two-oscillator results of Fig. 1. Indeed, this instability is beyond the scale of the figures in the large-coupling bottom row panels. The other type of instability, which they call a “collective instability,” is associated with the divergence of the mean $\langle x \rangle$ and hence of the second term in Eq. (16). The collective instability boundaries are shown as dashed curves in all panels of Fig. 6. Note that the two types of instability may occur simultaneously, as seen in the instability region overlap evident in the top row panels of the figure. We return to this point below. Note also that with increasing coupling the system becomes increasingly stable, as one might expect, and that the unstable be-

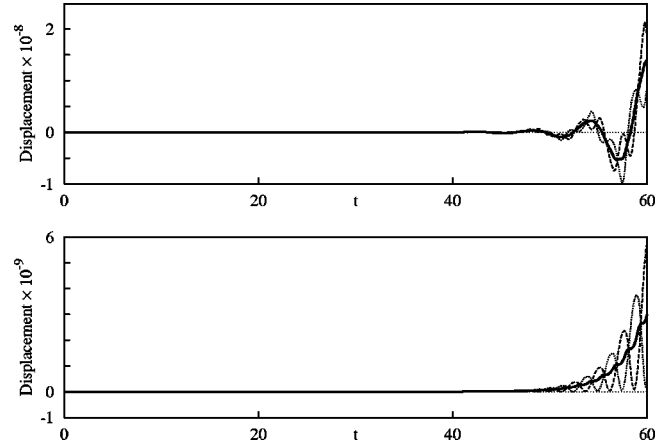


FIG. 7. Trajectories for the two-oscillator $\theta=\pi$ system for the parameters corresponding to the dark points in the upper right panel of Fig. 6: $\gamma/\omega_0=0.4$, $A=3$, and $k/\omega_0^2=4$. $r=0.25$ in the upper panel and 0.4 in the lower panel. The dashed curves are the displacement x_1 of one oscillator vs time, the dotted curves are the displacement x_2 of the other oscillator, and the thick solid curves represent the mean displacement $x=(x_1+x_2)/2$.

havior becomes primarily collective.

We wish to explore whether our two-oscillator model is able to capture at least some of the behavior of the infinite system. In particular, we would like to investigate whether features of the collective instabilities of the mean-field model are apparent in a system of only two oscillators with a fixed relative modulation phase. To make the comparison we also show in Fig. 6 the stability boundary for a single uncoupled oscillator (thin solid lines in left column) and for two coupled oscillators with relative modulation phase $\theta=\pi$.

We make the following assertions: the two-oscillator system with *any* value of θ captures features of the overlap region of “usual” and “collective” instabilities. The *purely* “usual” regions are captured most accurately by the $\theta=0$ system, and the *purely* “collective” regime is best captured by the two-oscillator system with $\theta=\pi$. It is therefore this latter system that most fully captures (with unexpected detail) the principal features of collective behavior of the mean-field model, and does so with increasing accuracy as the coupling between oscillators increases. We support these assertions, particularly the last one which is the one of most interest to us, with the results shown in Figs. 6 and 7.

Clearly, the $\theta=0$ system captures the full “usual” instability regime *exactly* since, as already stated, the “usual” instability is exactly the same as the “ r' instability.” This identity is not restricted to the square wave modulation but holds for any periodic modulation. However, the $\theta=0$ system does not capture the “collective” instability since the “ r' -instability” condition is that associated with a single parametric oscillator with the unshifted frequency ω_0 . Thus, for example, in the first panel of Fig. 6 the $\theta=0$ instability boundaries can be constructed from the combination of the dotted regimes and the thin solid lines (compare with the right lower panel of Fig. 1), whereas those of the mean-field system include the same dotted regimes but now the very different dashed regions. The left lower panel shows an even

greater difference between the $\theta=0$ two-oscillator model (whose “ r -instability” boundaries are independent of k) and the mean-field model (where the boundaries of the collective instability are sensitively dependent on k). Two coupled parametric oscillators with relative modulation phase $\theta=0$ therefore do not capture the collective features of the mean-field model.

Our assertion that the two-oscillator system with any θ contains elements of the “usual” instabilities in the mean-field model is simply a restatement of our earlier observation that “ r' instabilities” continue to appear even when one moves away from $\theta=0$ and all the way to $\theta=\pi$.

Consider now the two coupled oscillators with $\theta=\pi$. The stability boundaries are shown by the thick solid lines in the panels in the right column of Fig. 6. In the upper panel we observe that the first tongue approximates the region of “usual” mean-field instability (in the nonoverlapping regime) and that the remainder captures the collective instability boundary features surprisingly well [18]. We particularly point to the excellent fit of the leftmost boundary of this region. The agreement between the two models is even more dramatic in the lower panel, which corresponds to stronger coupling k . Again, the details are surprisingly well matched and the leftmost boundary of the region is captured essentially exactly.

To further support our analysis, and to gain a clearer understanding of the difference between “usual” and “collective” instabilities (which are both evidently already present in our two-oscillator system although the notion of a collective effect is not obvious in such a small system), we consider the motions that might characterize the instabilities. In the mean field system we conjecture that in the nonoverlapping “usual” instability regime the mean is zero, $\langle x \rangle = 0$, but each oscillator oscillates about zero with ever increasing amplitude. The motion in the nonoverlapping “collective” instability regime may involve an ever increasing mean with each oscillator oscillating about this moving mean with finite amplitude. This description is in accord with that of Bena and Van den Broeck [16]. The overlap regions may involve both an increasing mean and oscillations of ever increasing amplitude about the moving mean. We have not ascertained these conjectures in the mean-field system, but present results for the two-oscillator system that support this description.

Figure 7 shows trajectories for the two-oscillator $\theta=\pi$ system at the two points marked on the upper right panel of Fig. 6. The trajectories shown are those of each of the two oscillators as well as the mean trajectory. The upper panel is for parameter values in the unstable region that is *not* in the “collective” regime as identified by Bena and Van den Broeck [16]. It is tempting to associate this with the nonoverlapping “usual” instability of the mean-field model, an association that requires some caution. The figure indicates that not only does each oscillator and also the mean oscillate about zero, but all the trajectories, *including* the mean, appear to diverge. This behavior is that envisioned in our earlier discussion of the $\theta=0$ two-oscillator system in the regime where “ r instabilities” and “ r' instabilities” overlap, and is an indication that features of both kinds of instability

persist even at $\theta=\pi$. As we noted earlier, in a two-oscillator system with $\theta=\pi$ (and any odd parity periodic modulation) it is not possible to have either of these instabilities alone; our observations here illustrate this general conclusion for the specific model. The interpretation of the mean-field results in the language of “ r instabilities” and “ r' instabilities” requires a more detailed analysis of that model [19]. However, even with the results at hand it appears compelling that the “ r' -instability” contributions persist into the mean-field limit, becoming the nonoverlapping “usual” instability portion of the phase boundary portrait.

The lower panel of Fig. 7 is for parameter values in the nonoverlapping “collective” regime. The mean indeed increases essentially monotonically, and each oscillator oscillates about this increasing mean. It is interesting that the main feature of the “collective” instability, namely, an increasing mean displacement with individual oscillators oscillating about this mean, is already clearly captured by the two-oscillator model.

VI. CONCLUSIONS

We have studied two coupled parametric oscillators each with identical periodically modulated frequencies but with a phase difference θ between these modulations. This is a system intermediate between the well-known single parametric oscillator and the recently studied mean-field model of infinitely many mutually coupled oscillators [16]. Each of these extreme cases exhibits rich and intricate boundaries between stable and unstable behavior as the system parameters are varied, the main differences between the single oscillator and mean-field behavior being the occurrence of collective instabilities in the latter that of course have no counterpart in the former. Our principal motivation for this study has been to explore the seeds of collective behavior in a very small system and to understand the role of modulation phase differences in this collective behavior. Although we have explicitly explored a particularly simple (square wave) modulation, our most important conclusions extend beyond this simple case.

We found that a coupled system with in-phase modulations ($\theta=0$), although rich in its own right, does not mimic the collective behavior of the infinite system. It is nevertheless an interesting system because it can exhibit synchronous and antisynchronous behavior. Synchronous behavior involves the two oscillators moving together about zero (“ r instabilities”). The instability boundaries for this motion are identical to those of a single parametric oscillator of frequency ω_0 and are independent of coupling k since the spring connecting the oscillators is never disturbed. Antisynchronous behavior involves the two oscillators moving about zero but exactly in antiphase with one another (“ r' instabilities”). The stability boundaries for these motions are sensitive to k , and the system becomes more stable with increasing coupling. We noted that these latter instabilities are exactly those identified as “usual” instabilities in the mean-field model [16] and that they contribute to the instability boundaries in our two-oscillator model for any θ , not just for $\theta=0$. We also showed that damping shrinks the instability

regimes and smoothes the stability boundaries.

We showed that a change in θ can substantially modify the regions of parametric instability, and that these changes are strongly affected by the coupling between the oscillators. In general, increasing θ up to π provides greater stability but also leads to more intricate stability boundaries. An increase in k and/or γ also leads to increased stability. By projecting the instability regions onto the (k, θ) plane we were able to show (at least for the specific model considered here) that π -centered bands of stability arise for sufficiently large k and γ . We have thus identified all the trends of behavior in the two-oscillator model as each of the parameters is varied.

Our most interesting insights arise from a comparison of the two-oscillator results with the mean-field model [16]. As noted above, the “usual” instabilities of the mean field model are exactly our “ r ’ instabilities.” The interesting result is that the “collective” instabilities already appear in the

two-oscillator model with $\theta = \pi$. This statement is based on the great similarity of the stability boundaries of the mean field and two-oscillator systems, especially with increasing coupling, and the specific features of the oscillator trajectories that typify the motions in each of these unstable regimes. It is perhaps surprising that a two-oscillator model can capture so much of the mean-field collective behavior, and suggests that collective resonance in the latter may be dominated by phases quenched around π .

ACKNOWLEDGMENTS

We would like to thank C. Van den Broeck and R. Kawai for stimulating discussions. This work was supported in part by the National Science Foundation under Grant No. PHY-9970699.

-
- [1] B. van der Pol and M. J. O. Strutt, *Philos. Mag.* **5**, 18 (1928).
 - [2] L. D. Landau and E. M. Lifschitz, *Mechanics* (Pergamon Press, Oxford, 1969).
 - [3] V. I. Arnold, *Equations Différentielles Ordinaires* (Editions Mir, Moscow, 1974) [English translation: *Ordinary Differential Equations* (Springer-Verlag, Berlin, 1992)]; *Mathematical Theory of Classical Mechanics* (Springer-Verlag, Berlin, 1989).
 - [4] A. H. Nayfeh and D. T. Mook, *Nonlinear Oscillations* (Wiley, New York, 1979).
 - [5] C. Van den Broeck and I. Bena, in *Stochastic Processes in Physics, Chemistry and Biology*, edited by J. A. Freund and T. Poeschel, Lecture Notes in Physics Vol. 557 (Springer, Berlin, 2000), pp. 257–267.
 - [6] E. Kh. Akhmedov, *Pramana, J. Phys.* **54**, 47 (2000).
 - [7] M. Calvo, *Phys. Rev. B* **60**, 10 953 (1999).
 - [8] I. Zlatev, G. Huey, and P. J. Steinhardt, *Phys. Rev. D* **57**, 2152 (1998).
 - [9] J. W. Miles, *J. Fluid Mech.* **148**, 451 (1984); S. T. Milner, *ibid.* **225**, 81 (1991).
 - [10] S. Riyopoulos, *J. Plasma Phys.* **46**, 473 (1991); *Phys. Rev. Lett.* **68**, 3303 (1992).
 - [11] M. Calvo, *Phys. Rev. B* **55**, 10 571 (1997).
 - [12] N. V. Fomin, O. L. Shalaev, and D. V. Shantsev, *J. Appl. Phys.* **81**, 8091 (1997); K. Otsuka, D. Pieroux, W. Ting-Yi, and P. Mandel, *Opt. Lett.* **22**, 516 (1997).
 - [13] M. Schienbein and H. Gruler, *Phys. Rev. E* **56**, 7116 (1997); F. S. Prato, M. Kavaliers, A. P. Cullen, and A. W. Thomas, *Bioelectromagnetics* **18**, 284 (1997).
 - [14] D. Ballon *et al.*, *Magn. Reson. Med.* **39**, 789 (1998).
 - [15] R. Kobes and S. Peleš, e-print nonl-phys 0005005.
 - [16] I. Bena and C. Van den Broeck, *Europhys. Lett.* **48**, 498 (1999).
 - [17] J.-Y. Ji and J. Hong, *J. Phys. A* **31**, L689 (1998).
 - [18] According to recent results of R. Kawai (private communication) the apparent gap in the mean-field results does not exist but rather corresponds to a different type of instability [19].
 - [19] I. Bena, R. Kawai, C. Van den Broeck, M. Copelli, and K. Lindenberg (unpublished).